The Astrophysical Journal Supplement Series, 188:280–289, 2010 May doi:10.1088/0067-0049/188/1/280


# COSMIC CHRONOMETERS: CONSTRAINING THE EQUATION OF STATE OF DARK ENERGY. II. A SPECTROSCOPIC CATALOG OF RED GALAXIES IN GALAXY CLUSTERS

Daniel Stern[1], Raul Jimenez[2], Licia Verde[2], S. Adam Stanford[3,4], and Marc Kamionkowski[5]
[1] Jet Propulsion Laboratory, California Institute of Technology, 4800 Oak Grove Drive, Mail Stop 169-506, Pasadena, CA 91109, USA; stern@zwolfkinder.jpl.nasa.gov
[2] ICREA & Institute of Sciences of the Cosmos (ICC), University of Barcelona, Barcelona 08028, Spain
[3] Department of Physics, University of California, Davis, CA 95616, USA
[4] Institute for Geophysics and Planetary Physics, Lawrence Livermore National Laboratory, Livermore, CA 94551, USA
[5] California Institute of Technology, Mail Stop 350-17, Pasadena, CA 91125, USA
*Received 2009 July 19; accepted 2010 February 28; published 2010 May 4*

## ABSTRACT

We present a spectroscopic catalog of (mostly) red galaxies in 24 galaxy clusters in the redshift range $0.17 < z < 0.92$ obtained with the LRIS instrument on the Keck I telescope. Here we describe the observations and the galaxy spectra, including the discovery of three cD galaxies with LINER emission spectra, and the spectroscopic discovery of four new galaxy–galaxy lenses in cluster environments.

*Key words:* cosmology: observations

*Online-only material:* color figures, machine-readable table

## 1. INTRODUCTION

The nature of the physics driving cosmic acceleration is perhaps the biggest question facing physics today. Huge resources and large collaborations are now being amassed to determine the dark-energy equation-of-state parameter $w \equiv p/\rho$, relating the cosmic pressure $p$ to the energy density $\rho$ (in units of $c \equiv 1$). The value of $w$ could either be constant, as in the case of a cosmological constant ($w = -1$), or time dependent, as in the case of a rolling scale field or "quintessence" (Peebles & Ratra 1988; Caldwell et al. 1998). Any such behavior would have far-reaching implications for particle physics. The avenues that are now receiving the most attention are supernova searches, weak lensing, baryon acoustic oscillations, and cluster counts. However, none of these will be free from systematics, and it is still not clear which is the most promising approach. Most likely, multiple approaches will be required, and new ideas still need to be explored.

A new approach, proposed by Jimenez & Loeb (2002), is to measure the relative ages of luminous red galaxies, a probe that is particularly sensitive to the *variation* of $w(z)$ with redshift $z$. This method was demonstrated to work in Jimenez et al. (2003) with a set of low-redshift ($z \lesssim 0.25$) Sloan Digital Sky Survey (SDSS) luminous red galaxies from the sample of Eisenstein et al. (2001) supplemented with approximately two dozen moderate-redshift ($z \lesssim 1$) early-type galaxies observed with Keck. That work found $w \leqslant -0.8$ at the 68% confidence level. Using the SDSS sample to measure $dz/dt$ at $z \sim 0$, that work also derived an independent estimate for the Hubble constant, $H_0 = 69 \pm 12\,\mathrm{km\,s^{-1}\,Mpc^{-1}}$. Although this new cosmological test faces challenges from astrophysical uncertainties, these are not necessarily any more daunting than those associated with the more classical dark energy probes.

We describe here the results of a several night experiment with the Keck I telescope to obtain spectra of early-type galaxies in clusters at $0.2 \lesssim z \lesssim 1$. As demonstrated in Treu et al. (2005), the most massive early-type galaxies have the highest formation redshifts and are thus best suited to this experiment. Such galaxies are concentrated in galaxy clusters, with the additional benefit that *Galaxy Evolution Explorer* (*GALEX*) observations show that cluster elliptical galaxies have less UV emission than field elliptical galaxies (e.g., Schawinkski et al. 2007). This implies that cluster ellipticals have the lowest levels of "frosting" by recent star formation and thus are best suited for this experiment.

The multiplexing and unparalleled blue sensitivity of the Low Resolution Imaging Spectrometer (LRIS; Oke et al. 1995) on the Keck I telescope is a crucial aspect of this project, allowing simultaneous and accurate spectrophotometry of up to 20 cluster galaxies over a very wide spectral range, probing down to 2000 Å in the rest frame. The importance of the UV stellar breaks at rest frame 2640 Å and 2900 Å (B2640, B2900) was shown by Fanelli et al. (1992) and were used by Dunlop et al. (1996) and Spinrad et al. (1997) to determine the age of the high-redshift, quiescent radio galaxy LBDS 53W091. A comprehensive study by Dorman et al. (2003) dramatically shows that the rest-frame UV spectral region can be modeled accurately and, more importantly, that UV light (blueward of the 4000 Å region) can help to break the age–metallicity degeneracy.

Stern et al. (2010, Paper I) presents the cosmological results from this experiment and the derived constraints on both the equation of state of dark energy and the value of the Hubble "constant" as a function of redshift, $H(z)$. This paper (Paper II) presents the data in some detail, including target selection, observing strategy, data processing (Section 2), and a catalog of over 500 sources in the fields of 24 galaxy clusters out to $z \approx 1$ (Section 3.1). It is hoped that this resource will be useful for a number of other projects, such as more classic studies of galaxy and galaxy cluster evolution. In particular, we identified several interesting cD galaxies (Section 3.3) and we serendipitously found four new galaxy lenses (Section 3.4). Since most of the target samples are well-known clusters, some of these lenses already have *Hubble Space Telescope* (*HST*) imaging, and a more detailed analysis of the lens systems will be presented in L. A. Moustakas et al. (2012, in preparation). During the course of this program, we also observed and derived the mass of a stellar mass black hole in the Virgo globular cluster RZ 2109 (Zepf et al. 2008).

All but two of the galaxy clusters observed as part of this experiment were previously known. Thus, this work follows

**Table 1**
Cosmic Chronometer Observing Runs

| UT Date | % Dark | PI | Conditions/Comments |
|---|---|---|---|
| 2005 Feb 10 | 94 | Stanford | |
| 2007 Feb 17–18[a] | 100 | Kamionkowski | Weathered out |
| 2007 Aug 15–16[a] | 92–87 | Kamionkowski | Hurricane Flossie, two earthquakes, tsunami warning |
| 2007 Dec 17–18[a] | 48–40 | Kamionkowski | Poor conditions and bright moon |
| 2008 Jul 1[a] | 89 | Kamionkowski | |
| 2008 Sep 2–3[a] | 93–87 | Kamionkowski | First night lost to mechanical problems |
| 2009 Mar 2–3 | 62–52 | Harrison | Poor conditions and bright moon |

**Note.**
[a] Nights dedicated to cosmic chronometer experiment. Note the poor track record for the dedicated nights with only two successful nights out of nine allocations, thus traumatizing the PI during his first foray into observational astrophysics. Other observations were generally just a mask or two observed during nights focused on other programs.

on extensive work done by a variety of teams, as described in Section 2.1. The redshift catalog presented here compliments that work in two crucial manners. First, many of the sources presented here were targeted on the basis of their morphologies and/or colors, and thus do not have redshifts previously reported in the literature. As discussed in detail in Section 3.2, a comparison of our catalog to the NASA/IPAC Extragalactic Database (NED) finds that only 125 of the 514 of the sources reported here (e.g., 24%) have published redshifts—and of those sources, our redshifts differ significantly for only two of them. Second, the data presented here is of low resolution ($R \sim 600$) covering a wide wavelength range. Most previous catalogs of red galaxies in galaxy clusters, such as the ESO Distant Cluster Survey (EDisCS; Halliday et al. 2004; Milvang-Jensen et al. 2008), were obtained at higher resolution over a smaller wavelength range with less blue sensitivity.

## 2. DATA

Nine nights were awarded for this experiment between 2007 February and 2008 September (Table 1). Unfortunately, five of the nights were completely lost to weather (four nights) or instrument problems (one night). In particular, our two night observing run in 2007 August was lost to a combination of Hurricane Flossie (category four), two earthquakes (magnitudes 5.4 and 4.0), and a tsunami warning (due to a magnitude 8.0 earthquake in Peru). Of the four dedicated nights during which we obtained data, two (in 2007 December) suffered from both a bright (>50%) moon and poor conditions (thick cirrus and $\gtrsim 1\farcs5$ seeing). As shown in Table 1, we obtained a handful of additional observations during nights dedicated to other programs.

### 2.1. Target Selection

We targeted rich galaxy clusters in order to obtain an as large as possible sample of red galaxies over the redshift range $0.2 < z < 1$. Most of the clusters are well-known, rich X-ray clusters from a variety of samples such as the Abell (1958) catalog, the *ROSAT* Cluster Survey (RCS; Rosati et al. 1998) and the Massive Cluster Survey (MACS; Ebeling et al. 2001). In the redshift range $0.5 < z < 1$, only a few rich X-ray clusters are known (e.g., Ebeling et al. 2007), so we also targeted (and confirmed) two of the richest *Spitzer* mid-infrared selected cluster candidates from the Infrared Array Camera (IRAC) Shallow Cluster Survey (Eisenhardt et al. 2008). Many of the targeted clusters were also observed in the near-infrared cluster survey of Stanford et al. (2002), which provided a valuable and consistent astrometric resource for slit mask designs. The list of clusters targeted is presented in Table 2.

The galaxy cluster sample was chosen to meet the competing demands of providing a good distribution of cluster redshifts for the cosmological experiment, a good right ascension distribution for the assigned nights, as well as a good right ascension distribution of brighter clusters to observe during poor conditions. Once a cluster was chosen for observation, selecting early-type galaxy cluster members with which to fill the slit masks was an intensive, but non-uniform, process. We did not have deep, photometric, multiband imaging of most of our heterogeneous cluster sample, and thus were unable to identify a magnitude- or color-limited sample of candidate cluster members.

Instead, we populated our masks with a very heterogeneous set of sources. First, we relied on NED to identify known cluster members in the literature. For many clusters, we were able to spectroscopically target cluster members that had no known signatures of star formation or an active galactic nucleus (AGN). Some clusters also had published lists of candidate members based on either morphology or color (e.g., Stanford et al. 2002). For the Boötes clusters in the IRAC Shallow Survey (Eisenhardt et al. 2004; Ashby et al. 2009), photometric redshifts based on optical through mid-infrared data were used to select candidate early-type cluster members (Brodwin et al. 2006). Many of the clusters also had publicly available images in the *HST* archive from which we were able to morphologically and/or color select early-type galaxies, at least for the central portions of our slit masks. Since the most massive early-type galaxies have the highest formation redshifts (e.g., Treu et al. 2005), we biased our sample to the brightest candidate cluster members. By publicly releasing the results for our mongrel spectroscopic sample, we hope that future studies can use these results to study, for example, how spectroscopic properties (e.g., ages, presence of emission lines) depend on morphology, absolute magnitude, or distance from the cluster center.

An additional challenge of the myriad source lists used to populate the masks was that each source list was based on a slightly different astrometric reference frame. For the mask designs, we required consistent astrometry for all candidates across the full $5' \times 7'$ LRIS field, including a minimum of three alignment stars brighter than $B \sim 20$. For the lower redshift clusters, publicly available images from the Palomar Sky Survey or SDSS proved sufficient. For the higher redshift clusters, however, candidate cluster members were often too faint to provide robust centroiding in those shallow data. For many of these clusters we were able to obtain images with the

**Table 2**
Galaxy Clusters Observed

| Galaxy Cluster | R.A. | Decl. | Redshift | UT Date | P.A. (deg) | Comments |
|---|---|---|---|---|---|---|
| MS 0906.5+1110 | 09:09:12.7 | +10:58:29 | 0.172 | 2005 Feb 10 | −70.1 | |
| MS 1253.9+0456 | 12:56:00.0 | +04:40:00 | 0.230 | 2008 Jul 1 | 42.7 | |
| Abell 1525 | 12:21:57.8 | −01:08:03 | 0.260 | 2007 Dec 18 | 122.6 | |
| MS 1008.1−1224 | 10:10:32.3 | −12:39:52 | 0.301 | 2007 Dec 17 | 115.5 | |
| CL 2244−0205 | 22:47:13.1 | −02:05:39 | 0.330 | 2007 Dec 17–18 | −124.4 | Poor conditions |
| Abell 370 | 02:39:53.8 | −01:34:24 | 0.374 | 2007 Dec 18 | 70.0 | |
| MACS J1720.2+3536 | 17:20:12.0 | +35:36:00 | 0.389 | 2008 Sep 3 | 69.6 | |
| CL 0024+16 | 00:26:35.7 | +17:09:45 | 0.394 | 2007 Dec 18 | −5.5 | |
| MACS J0429.6−0253 | 04:29:41.1 | −02:53:33 | 0.400 | 2008 Sep 3 | 46.3 | |
| MACS J0159.8−0849 | 01:59:00.0 | −08:49:00 | 0.405 | 2008 Sep 3 | 17.6 | |
| Abell 851 | 09:43:02.7 | +46:58:37 | 0.405 | 2007 Dec 17 | 60.3 | |
| GHO 0303+1706 | 03:06:19.1 | +17:18:49 | 0.423 | 2005 Feb 10 | −60.0 | |
| MS 1621.5+2640 | 16:23:00.0 | +26:33:00 | 0.428 | 2008 Jul 1 | 27.9 | |
| MACS J1621.3+3810 | 16:21:24.8 | +38:10:09 | 0.465 | 2008 Sep 3 | −47.1 | |
| MACS J0257.1−2325 | 02:57:09.1 | −23:26:06 | 0.505 | 2008 Sep 3 | 51.8 | |
| MS 0451.6−0306 | 04:54:10.8 | −03:00:57 | 0.539 | 2005 Feb 10 | −39.1 | |
| MS 0451.6−0306 | 04:54:10.8 | −03:00:57 | 0.539 | 2007 Dec 17–18 | −83.4 | |
| Boötes 10.1 | 14:32:06.0 | +34:16:47 | 0.544 | 2008 Sep 3 | 54.5 | |
| CL 0016+16 | 00:18:33.5 | +16:25:15 | 0.545 | 2007 Dec 18 | 139.4 | Poor conditions |
| MACS J2129.4−0741 | 21:26:46.9 | −07:54:36 | 0.570 | 2008 Jul 1 | 75.0 | |
| MACS J0025.4−1222 | 00:25:09.4 | −12:22:37 | 0.578 | 2008 Jul 1 | −25.9 | |
| MACS J0647.7+7015 | 06:47:50.5 | +70:14:55 | 0.591 | 2009 Mar 2 | −71.1 | Mask 1 |
| MACS J0647.7+7015 | 06:47:50.5 | +70:14:55 | 0.591 | 2009 Mar 3 | −95.5 | Mask 2 |
| MACS J0744.8+3927 | 07:44:52.5 | +39:27:27 | 0.697 | 2009 Mar 2 | 91.7 | Mask 1 |
| MACS J0744.8+3927 | 07:44:52.5 | +39:27:27 | 0.697 | 2009 Mar 3 | 97.6 | Mask 2 |
| RCS 2318+0034 | 23:18:31.5 | +00:34:18 | 0.756 | 2008 Sep 3 | −26.1 | |
| Boötes 10.8 | 14:32:06.0 | +34:16:47 | 0.921 | 2008 Jul 1 | −25.0 | |

**Note.** Cluster positions are in the J2000 coordinate system.

roboticized Palomar 60″ (P60) telescope (Cenko et al. 2006) which is equipped with an SITe 2048 × 2048 pixel CCD with a pixel scale of 0.″378 pixel$^{-1}$ and a 12.′9 × 12.′9 field of view. For such clusters, we observed two bands chosen to straddle the 4000 Å break (D4000) at the cluster redshift. Multi-band images, either from the P60 or the public data sets, provided an additional sample of visually identified red sources near the cluster with which to populate the masks. Note that due to the geometric constraints from the mask designs, masks inevitably also included targets which were unlikely to be early-type cluster members.

### 2.2. Observing Strategy

The key goal of this program was to provide high signal-to-noise ratio (S/N), wide wavelength coverage spectroscopy of a large number of early-type galaxies at moderate redshifts. These spectra were then modeled to derive the ages of the galaxy stellar populations. Since rest-frame UV light probes the youngest, most massive stars in a galaxy, blue sensitivity is crucial for this experiment. Of all the optical spectrographs on 8–10 m class telescopes currently available, LRIS on the Keck I telescope is unique in being the only dual-beam multi-object spectrograph, thus providing sensitive observations across the entire optical window ($\lambda \sim 3200$ Å–1 $\mu$m).

LRIS provides spectra of approximately 25 sources simultaneously across a $\sim 5' \times 7'$ field of view, with a dichroic splitting the light between the blue and red channels. For most of the observations, we observed the same mask with two different dichroics, thereby ensuring that the final spectra have no gaps which might compromise the stellar population modeling. Only the three masks observed in 2005 February were observed with a single dichroic. LRIS has an ample set of dichroics to choose from; we consistently selected dichroics that avoided the rest-frame 4000 Å spectral region which includes import stellar population diagnostics (e.g., [O II] $\lambda$3727, D4000 and the Balmer break).

We obtained the blue channel data with the 400 lines mm$^{-1}$ grism, which has a central wavelength of 3400 Å and a spectral range of 4450 Å. We obtained the red channel data with the 400 lines mm$^{-1}$ grating, which has a central wavelength of 8500 Å and a spectral range of 3800 Å. Combining the blue and red channel data from the two dichroic settings, sources typically had final spectra which spanned the entire ∼3200 Å −1 $\mu$m optical window, albeit with higher noise at the short and long wavelength extremes. Based on analysis of sky lines, sources filling the 1.″5 wide slitlets used for these observations have resolution $\lambda/\Delta\lambda \sim 500$ and ∼650 for the blue and red channels, respectively. Standard stars from Massey & Gronwall (1990) were observed with the same instrument configuration for the purposes of spectrophotometric calibration.

Observations were generally obtained with two dithered exposures per dichroic configuration with typical integration times of 900 s to 1800 s, depending on the cluster redshift and observing conditions. This allowed both improved cosmic ray rejection and, by pair-wise subtraction of the red images, removal of the fringing which strongly affects the long wavelength ($\lambda \gtrsim 7200$ Å) LRIS data. This required minimum slitlet lengths of approximately 10″. Since LRIS has an atmospheric dispersion corrector, mask position angles were optimized based on the cluster orientation and no special attention was necessary to align the masks with the parallactic angle.

### 2.3. Reductions

We processed the spectroscopic data with BOGUS,[6] which is an IRAF[7] routine designed for two-dimensional processing of multislit data and was written by D. Stern, A. Bunker, and S. A. Stanford. After gain and overscan correction of the raw two-dimensional images, BOGUS basically splits the mask into individual slitlets and processes each slitlet using standard optical long-slit techniques. After flattening the spectrum with either dome flats (recommended for the red channel of LRIS) or twilight flats (recommended for the blue channel of LRIS), cosmic rays are identified from unsharp masking of the images, sky lines are subtracted using a low order polynomial fit to each column, and images are shifted by integer pixels in the spatial and dispersion directions and recombined. For the red channel data, an additional step of pair-wise image subtraction improves fringe subtraction at long wavelength. As a final step, BOGUS shifts each of the slitlets to roughly align them in the wavelength direction. This both simplifies wavelength calibration and the rapid visual identification of spectroscopically confirmed cluster members.

After the two-dimensional processing provided by BOGUS, we extracted the spectra using 1.″5 wide extraction traces using the APALL procedure within IRAF. We extracted arc lamps in an identical manner and used them to do a first pass wavelength calibration of the data. This typically relied on a fourth order polynomial wavelength solution, providing a ≈0.5 Å rms to the blue channel of LRIS and a ≈0.1 Å rms to the red channel of LRIS. As a final step in the wavelength calibration, these lines were shifted based on the sky lines and we conservatively estimate that the wavelength solutions are robust to better than 1 Å. We flux calibrated the spectra using spectrophotometic standards observed during each observing run.

At this point, each slit mask target generally has four spectra: the blue and red channel observations for each of the two dichroics. To combine the spectra into a single, final spectrum for the stellar population synthesis analysis, we did the following. Spectra were trimmed at their blue and red ends to restrict coverage to regions of more robust spectrophotometry. Generally, wavelengths blueward of observed ∼3500 Å were removed due to their lower signal to noise. Pixels within 50 Å of the dichroics were eliminated. At long wavelength, spectral trimming depended on individual analysis of the spectra. Fainter targets and/or targets observed with no dithering often showed significant systematic glitches in their long wavelength data, and thus were trimmed at relatively blue wavelengths (∼7500 Å). Other sources had robust spectra out to ∼9500 Å. Since the observations were not all obtained in photometric conditions, the final combination of the spectra required multiplicative scaling of their calibrated spectra, which generally was normalized to the blue channel data with the longer wavelength dichroic. We derived statistical error spectra assuming Poisson uncertainties of sky plus science target counts within the extraction regions. For observations where an extra step of fringe subtraction was applied, the error spectra were increased by $\sqrt{2}$ to account for the statistical noise hit from that procedure. During the final step of combining the multiple spectra (which generally were all obtained with the same exposure time), the error spectra were averaged and scaled down by $\sqrt{2}$. The final spectra had a typical S/N ≈ 12–15 per 3 Å resolution element.

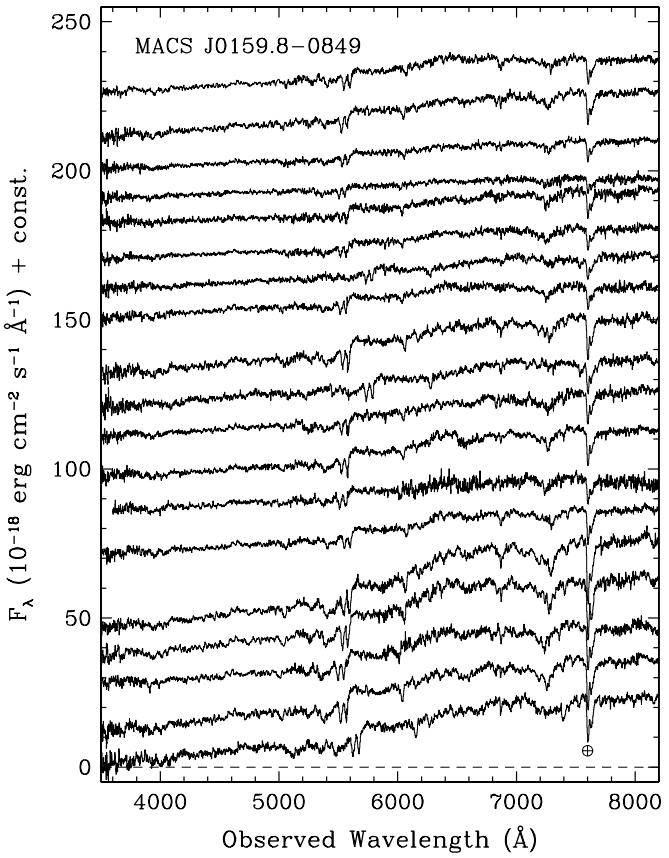


**Figure 1.** Results of a typical mask, MACS J0159.8−0849 at $z = 0.405$, observed on UT 2008 September 3. Telluric *A*-band absorption is indicated.

## 3. RESULTS

### 3.1. Spectra of Galaxies in Clusters

Figure 1 presents the results from the a typical mask: MACS J0159.8−0849 at $z = 0.405$, observed on UT 2008 September 3. Nearly 20 early-type cluster members were obtained simultaneously, each clearly showing an evolved stellar population with strong Ca H and K absorption and a prominent D4000 break. Figure 2 averages spectra of cluster members for masks observed in late 2008 and shows a clear sequence with redshift: clusters at lower redshift contain older stellar populations, recognized from their redder spectral energy distributions (SEDs) and larger D4000 breaks.

Table 3 and Figure 3 present the results from the spectroscopy. For most sources, redshift determinations are based on Gaussian fits to emission features such as Ly$\alpha$, [O II], H$\beta$, [O III], and H$\alpha$, and/or based on Gaussian fits to absorption features such as Ca H, Ca K, *G*-band, Mg Ib, and NaD. For a few low-quality spectra, redshifts were estimated based on the location of a strong spectral break assumed to be D4000. The spectra are classified on the basis of both their quality and their spectral class. Quality "A" indicates very reliable redshifts based on multiple, well-observed features. Quality "B" indicates reliable redshifts, but often based on a single feature—e.g., the single emission feature detected is assumed to be either Ly$\alpha$ or [O II], or a break is identified, but with insufficient fidelity to derive a precision redshift. Quality "B" redshifts are likely correct,

[6] Available upon request from the first author.

[7] IRAF is distributed by the National Optical Astronomy Observatories, which are operated by the Association of Universities for Research in Astronomy, Inc., under cooperative agreement with the National Science Foundation.

**Table 3**
Spectroscopic Results

| Object ID | R.A. | Decl. | Redshift | Quality | Class | Notes |
|---|---|---|---|---|---|---|
| CL0024 gxy07 | 00:26:24.620 | +17:13:33.510 | 0.246 | A | S | [O II], H$\alpha$; Czoske et al. (2001) |
| CL0024 gxy26 | 00:26:25.420 | +17:13:22.812 | 0.399 | A | E | MgB; Czoske et al. (2001) |
| CL0024 g202p | 00:26:26.029 | +17:11:16.559 | 0.392 | A | E+S | [O II], CaHK; Czoske et al. (2001) |
| CL0024 g215p | 00:26:27.117 | +17:12:26.082 | 0.398 | A | E | CaHK; Moran et al. (2007b) |
| CL0024 gxy21 | 00:26:27.709 | +17:13:49.797 | 0.395 | A | S | [O II]; Czoske et al. (2001) |
| CL0024 g226p | 00:26:27.956 | +17:11:37.879 | 0.394 | A | E | CaHK; Czoske et al. (2001) |
| CL0024 gxy06 | 00:26:28.381 | +17:12:46.550 | 0.397 | B | E | CaHK; Czoske et al. (2001) |
| CL0024 gxy04 | 00:26:31.029 | +17:12:09.808 | 0.0 | A | ⋆ | M-star |
| CL0024 gxy03 | 00:26:31.392 | +17:10:56.131 | 0.397 | A | E | CaHK; Moran et al. (2007b) |
| CL0024 g334p | 00:26:34.210 | +17:10:09.844 | 0.387 | A | E | CaHK; Czoske et al. (2001) |
| CL0024 g338p | 00:26:34.348 | +17:10:22.630 | 0.388 | A | E | CaHK; Moran et al. (2007b) |
| CL0024 gxy08 | 00:26:34.626 | +17:08:10.100 | 0.0 | A | ⋆ | M-star |
| CL0024 g353p | 00:26:34.838 | +17:09:19.273 | 0.398 | A | E | CaHK; Dressler & Gunn (1992); Moran et al. (2007b) |
| CL0024 g362p | 00:26:35.018 | +17:09:39.309 | 0.399 | A | E | CaHK; Dressler & Gunn (1992) |
| CL0024 g363p | 00:26:35.206 | +17:09:49.238 | 0.389 | A | E | CaHK; Czoske et al. (2001) |
| CL0024 g383p | 00:26:36.140 | +17:08:27.616 | 0.402 | A | E | CaHK; Czoske et al. (2001) |
| CL0024 gxy02 | 00:26:36.250 | +17:10:00.925 | 0.390 | A | E | CaHK; Czoske et al. (2001) |
| CL0024 gxy09 | 00:26:37.313 | +17:07:50.647 | 0.392 | A | E | CaHK; Czoske et al. (2001) |
| CL0024 gxy10 | 00:26:38.418 | +17:07:31.566 | 0.392 | A | E | CaHK; Czoske et al. (2001) |
| CL0024 g458p | 00:26:41.879 | +17:10:45.495 | 0.390 | A | E | CaHK; Czoske et al. (2001) |

**Notes.** The full table of 514 sources is included in the electronic version of this paper. Positions are in the J2000 coordinate system. Typical redshift uncertainties are ±0.002. Only quality "A" (very reliable) and "B" (reliable) redshifts are presented. Spectroscopic classes are E (elliptical, or early-type spectrum), S (spiral, or late-type spectrum), AGN (quasar), and ⋆ (Galactic star).

(This table is available in its entirety in a machine-readable form in the online journal. A portion is shown here for guidance regarding its form and content.)

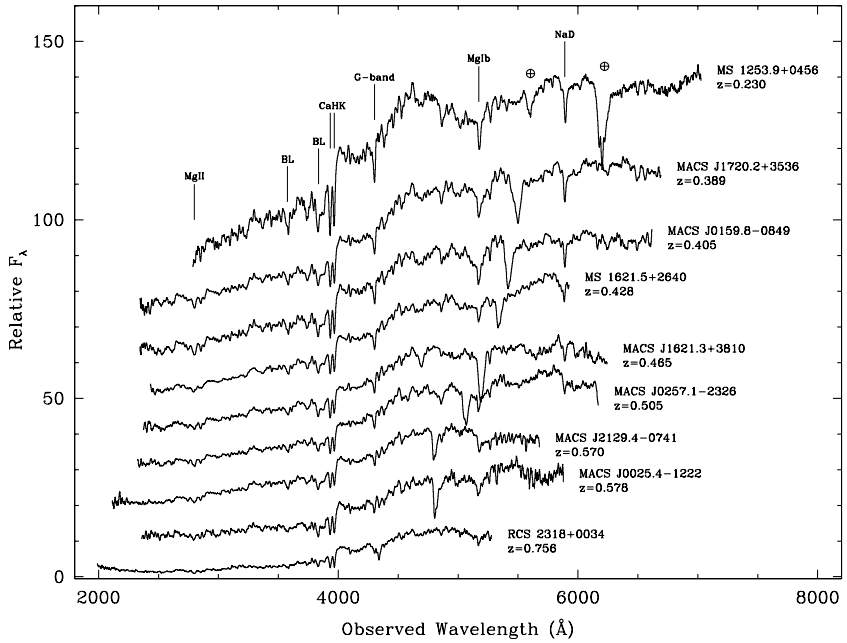


**Figure 2.** Averaged spectra of cluster ellipticals from the observing runs in 2008 July and September, plotted as a function of redshift. Primary spectral features are indicated. Telluric *A*-band (7600 Å) and *B*-band (6880 Å) absorption are indicated for the lowest redshift cluster (top); these features shift to shorter rest-frame wavelengths for the higher redshift clusters.

though an occasional line misidentification is possible. Based on a comparison of redshifts derived from multiple features, quality "A" redshifts are conservatively estimated to have uncertainties of 0.002 in redshift. Assuming the features are correctly identified, quality "B" redshifts will have comparable uncertainties, though quality "B" redshifts derived from spectral breaks (e.g., without Gaussian fits to emission or absorption features) are assumed to have uncertainties of 0.004 in redshift. For consistency, we assume the pessimistic redshift uncertainty for all quality "B" redshifts in Table 3. Our internal processing also included quality "C" (tentative) and "F" (uncertain) flags, though such sources are omitted from Table 3.

The spectral quality assessments are qualitative, not quantitative. However, using similar spectroscopic assessments for a large set of deep Keck spectra in the Great Observatories Origins Deep Survey (GOODS) fields, D. Stern et al. (2012, in preparation) finds that quality "A" redshifts were self-consistent ∼95% of the time. Mistakes were generally due to target/serendip misidentifications in those very deep spectra, an issue which is less likely to arise in the shallow data

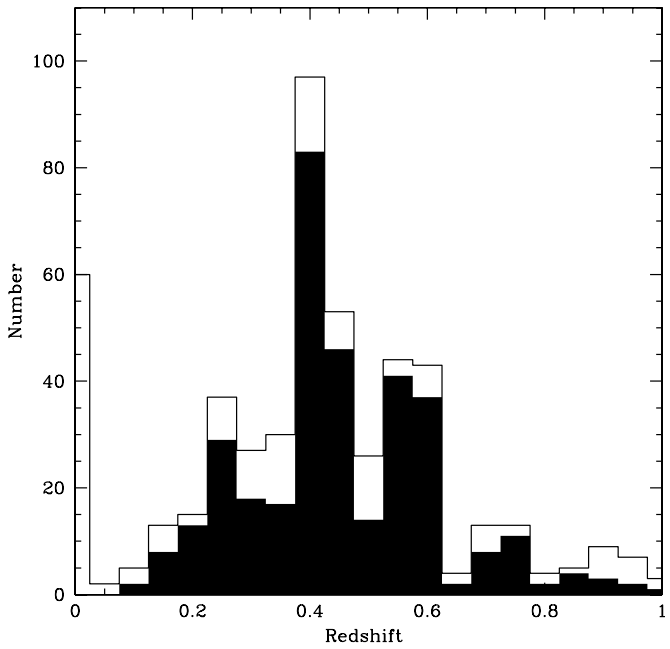


**Figure 3.** Histogram of redshifts derived from this program. The open histogram shows all 514 sources, while the solid histogram only shows the highest quality (quality "A") absorption-line (class "E") redshifts. Note the high fraction of early-type galaxies from this program, much higher than would be found in a field galaxy survey.

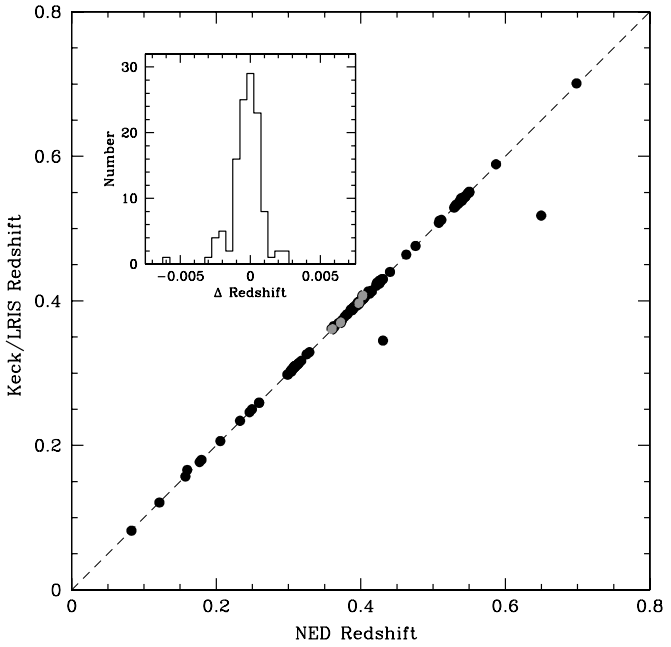


**Figure 4.** Comparison of our Keck/LRIS redshifts for the 125 galaxies with published redshifts in NED. Quality A (B) redshifts are shown in black (gray). The two clear outliers are gxy20 in Abell 851 and g122372 in MS 1621.5+2640, which are likely due to either source confusion or errors in the literature. Both are discussed in detail in Section 3.2. The inset histogram shows the distribution of $\Delta z \equiv z_{\rm NED} - z_{\rm Keck}$ for the 121 quality A redshifts: omitting the two outliers, $\langle \Delta z \rangle = -0.0003$ and $\sigma_{\Delta z} = 0.0011$.

presented here. Quality "B" redshifts appeared problematic ∼15% of the time, though, again, mistakes were generally due to source confusion in those deep data. The redshift uncertainties quoted above are consistent, or slightly pessimistic, compared to the results of D. Stern et al. (2012, in preparation). More assuringly, Section 3.2 and Figure 4 compare our results to the literature. Ignoring two discrepant galaxies which we suggest are due to source confusion or errors in the literature (see Section 3.2), we find that our redshifts are quite robust: the average offset between our redshifts and published redshifts is 0.0003 (e.g., beyond the accuracy of our redshifts) and has a standard deviation of 0.0011 (e.g., almost a factor of 2 better than the 0.002 redshift uncertainties we assume for our quality A redshifts; note, however, that published redshifts are likely to be for brighter galaxies).

We assign each of the spectra one of four spectroscopic classes (or a hybrid of these classes). Spectroscopic class "E" refers to early-type or elliptical galaxy spectra, showing only spectral breaks and absorption lines. Such sources were the primary goal of this program. Spectral class "S" refers to late-type or spiral galaxy spectra, showing emission lines such as [O II], H$\beta$, [O III], and H$\alpha$, typical of star-forming galaxies. We identified several stars during this program, tabulated as spectral class "⋆." Many are late-type stars of spectral class M, mistakenly targeted on the basis of their red colors mimicking that of moderate-redshift early-type galaxies. A handful of early-type stars were also serendipitously observed. Finally, we observed a handful of active galaxies, listed as spectral class "AGN."

In total, we obtained 514 redshifts in galaxy cluster fields during this program, of which the vast majority (484, or 94%) are quality "A" (Figure 3). For the targeted cluster early-type galaxy sample, we obtained a total of 363 sources, of which 341 (94%) are quality "A." Note that just because a source is of quality "A" does not ensure that it will be useful for the cosmic chronometer experiment (Paper I). A target might have a reliable redshift due to the detection of specific features, while the continuum might be of low S/N due to poor fringe subtraction, contamination from a nearby source, or simply due to the observing conditions.

### *3.2. Comparison to the Literature/Notes*

This subsection includes notes on individual clusters, focused on a comparison of our spectroscopic results to spectroscopic results in the NED archive (using a 5″ search radius in 2010 February).

*MS 0906.5+1110* ($z = 0.172$). Several of the targets in this cluster were identified as potential cluster members on the basis of their optical through near-infrared SEDs in Stanford et al. (2002). Two galaxies have spectroscopic redshifts in the SDSS archive which match our redshifts to the accuracy of our data (e.g., $\Delta z < 0.0005$). One target, gxy14, was previously published in the catalog of Paturel et al. (2000) with $\Delta z = -0.006$ relative to our derived redshift (quality "A"). A visual re-inspection confirms the Keck redshift, suggesting either that the earlier redshift is inaccurate or the redshift discrepancy is due to source confusion.

*MS 1253.9+0456* ($z = 0.230$). Several of the targets in this cluster were identified as potential cluster members on the basis of their optical through near-infrared SEDs in Stanford et al. (2002). Two galaxies have spectroscopic redshifts in the SDSS archive which match our redshifts to high accuracy ($\Delta z \leqslant 0.001$).

*Abell 1525* ($z = 0.260$). Several of the targets in this cluster were identified as potential cluster members on the basis of their optical through near-infrared SEDs in Stanford et al. (2002). Two galaxies have spectroscopic redshifts in the SDSS and/or 2dFGRS archives which match our redshifts to high accuracy ($\Delta z \leqslant 0.0006$). This cluster is part of the maxBCG sample of Koester et al. (2007).

*MS 1008.1−1224* ($z = 0.301$). This cluster, which was also part of the Stanford et al. (2002) sample, was studied

extensively as part of the Canadian Network for Observation Cosmology Cluster Redshift Survey (CNOC1; Yee et al. 1998). We targeted 21 galaxies from CNOC1, finding very similar results for 20 of the sources ($\Delta z \lesssim 0.001$). The one apparent discrepancy, g1142x, is likely due to source confusion. We associate this source with a Galactic star (quality "A"), while the cluster member at $z = 0.310$ found by Yee et al. (1998) is likely associated with the 4.″4 offset source at 10:10:17.68, −12:39:03.6 (J2000). The CNOC1 astrometry, which is slightly offset from our own, places g1142x between these two sources.

*CL 2244−0205* ($z = 0.330$). Several of the targets in this cluster were identified as potential cluster members on the basis of their optical through near-infrared SEDs in Stanford et al. (2002). None of the sources tabulated here have spectroscopic redshifts in NED.

*Abell 370* ($z = 0.374$). This famous cluster has been the subject of numerous spectroscopic studies (e.g., Soucail et al. 1988; Ziegler & Bender 1997; Dressler et al. 1999). Our spectroscopic results are fully consistent with the published literature ($\Delta z \lesssim 0.002$).

*MACS 1720.2+3536* ($z = 0.389$). Though many of the targets in this field are in the SDSS photometric catalog, no redshifts are available through NED.

*CL 0024+16* ($z = 0.394$). This famous cluster has been the subject of numerous spectroscopic studies (e.g., Dressler & Gunn 1992; Czoske et al. 2001; Moran et al. 2005, 2007b). All 18 galaxies confirmed in this cluster have redshifts available through NED. In all cases, our redshifts agree with the published values ($\Delta z \leqslant 0.002$). Our one apparent discrepancy is "gxy04" which we classify as a Galactic M-star, while Moran et al. (2005) report a cluster member 2.″6 to the NE.

*MACS 0429.6−0253* ($z = 0.400$). None of the targets in this cluster are registered in NED.

*MACS 0159.8−0849* ($z = 0.405$). Three galaxies have spectroscopic redshifts in the SDSS archive which match our redshifts to the accuracy of our data (e.g., $\Delta z < 0.0005$).

*Abell 851* ($z = 0.405$). This famous cluster has been the subject of numerous spectroscopic studies (e.g., Dressler & Gunn 1992; Belloni et al. 1995; Belloni & Roser 1996; Dressler et al. 1999). The work by Belloni and collaborators relied on narrow- and broadband filters to obtain low resolution spectra (e.g., photometric redshifts), and generally are consistent with our true spectroscopic results ($\Delta z \lesssim 0.05$), though Belloni & Roser (1996) infer a redshift of $z = 0.530$ for s1370x, while we derive $z = 0.157$ based on multiple emission features. In comparison to the work of Dressler and collaborators, our cluster member redshifts are generally quite consistent ($\Delta z \lesssim 0.002$), though our quality "B" redshift for g159x is offset by $\Delta z = 0.004$ from the results of Dressler & Gunn (1992) and we identify background galaxy gxy20 to be at $z = 0.518$ based on multiple emission line features (e.g., [O II], H$\beta$, [O III]) while Dressler et al. (1999) identify this apparently isolated source (CL 0939 082 in their catalog) to be at $z = 0.6497$ based on the claimed detection of [O II] and Balmer absorption features (spectroscopic quality 2, on a scale of 1 to 5 with one indicating the most confident redshifts). The quasar in this field ("gxy23") was also identified by the *XMM-Newton* Medium Sensitivity Survey (Barcons et al. 2007) with a comparable redshift ($\Delta z = 0.002$). In the numerical comparison of our spectroscopic results to results in the literature (discussed in Section 3.1), neither the quasar nor the photometric redshifts of Belloni et al. were included when calculating the average accuracy of our spectroscopic redshifts.

*GHO 0303+1706* ($z = 0.423$). No redshifts of targets in this cluster are available through NED.

*MS 1621.5+2640* ($z = 0.428$). This cluster was extensively studied as part of the CNOC survey, with spectroscopic results for 20 of our targets presented in Ellingson et al. (1997). We find very similar results for 19 of these galaxies, with $\Delta z \lesssim 0.001$. The one discrepant source, g122372p, is an early-type galaxy at $z = 0.345$ (quality A) according to our results, but is listed as a cluster member at $z = 0.431$ in Ellingson et al. (1997). Our shallow P60 image shows g122372p to be an isolated source, suggesting that the CNOC result is either in error or due to confusion with a faint source. One additional galaxy has a spectroscopic redshift in the SDSS archive with a redshift matching our results. Finally, we note that Nakamura et al. (2006) present MS1621 P1 05_A at $z = 0.630$ which is slightly ($\sim 2''$) offset relative to our g101444p at $z = 0.425$ (quality A; matches CNOC results). The background galaxy is faintly visible in our P60 image, and is clearly resolved in the deep Subaru/FOCAS image presented in Nakamura et al. (2006).

*MACS 1621.3+3810* ($z = 0.465$). One galaxy has a spectroscopic redshift in the SDSS archive. The results match with $\Delta z = 0.001$.

*MACS 0257.1−2325* ($z = 0.505$). None of the targets in this cluster are registered in NED.

*MS 0451.6−0306* ($z = 0.539$). This cluster was extensively studied by the CNOC survey (Ellingson et al. 1998) and by Moran et al. (2007a, 2007b), with spectroscopic results for the majority of the galaxies observed previously published in those works. In all cases, our results are consistent with the published results ($\Delta z \lesssim 0.001$).

*Boötes 10.1* ($z = 0.544$). One foreground galaxy (g056; $z = 0.121$) has a fully consistent redshift available from the SDSS archive ($\Delta z < 0.0005$).

*CL 0016+16* ($z = 0.545$). This cluster, also known as MS 0015.9+1609, was extensively studied by Dressler & Gunn (1992) and the CNOC survey (Ellingson et al. 1998). Four of our targets were previously published by those works, and in all cases the derived redshifts are fully consistent ($\Delta z < 0.001$).

*MACS J2129.4−0741* ($z = 0.570$). One cluster member (g001) has a spectroscopic redshift in the SDSS archive. The results match with $\Delta z < 0.002$.

*MACS J0025.4−1222* ($z = 0.578$). None of the targets in this cluster are registered in NED.

*MACS J0647.7+7015* ($z = 0.591$). No redshifts of targets in this cluster are available through NED.

*MACS J0744.8+3927* ($z = 0.697$). The redshift of the cD galaxy was also obtained by SDSS, with a result matching our own ($\Delta z = 0.002$).

*RCS 2318+0034* ($z = 0.756$). No redshifts of targets in this cluster are available through NED.

*Boötes 10.8* ($z = 0.921$). No redshifts of targets in this cluster are available through NED.

In summary, approximately a third of our cluster sample are well-known fields with many of our redshifts previously published in the literature (e.g., MS 1008.1−1224, Abell 370, CL 0024+16, Abell 851, MS 1621.5+2640, MS 0451.6−0306, and CL 0016+16). We present a total of 514 spectroscopic redshifts in this catalog, of which 125 (24%) repeat results in the literature. Two discrepancies are found, possibly due to source confusion, while the other sources validate the accuracy of our redshifts (Figure 4). We present spectroscopic redshifts for a total of 363 early-type galaxies, of which 254 (70%) are not previously in the literature.

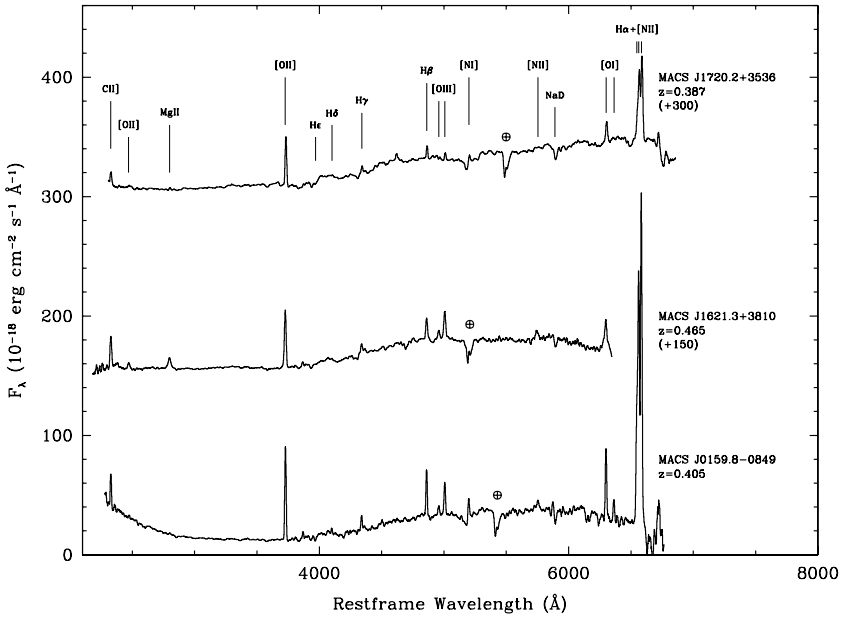


**Figure 5.** Spectra of three cluster cD galaxies showing strong emission lines, typical of LINERs.

### *3.3. cD Galaxies*

Three of the central cD galaxies observed during this program have interesting spectra showing multiple emission lines superposed on a red, evolved stellar population (Figure 5; see also Edge et al. 2003). The spectra are similar to that of NGC 1275, the central galaxy in the Perseus cluster (e.g., Sabra et al. 2000), and are clearly classified as LINER-like spectra. Indeed, log ([O I] 6300/[O III] 5007) ranges from 0.13 to 0.59 for the three galaxies, which is much larger than typical of star-forming galaxies in the SDSS (Brinchmann et al. 2008). All three galaxies are detected by the Faint Images of the Radio Sky at Twenty cm survey (FIRST; Becker et al. 1995), with 1.4 GHz flux densities of 31.43 mJy, 5.59 mJy, and 16.75 mJy for MACS J015949.3−84958, MACS J162124.7+381008, and MACS J172016.7+353626, respectively.

While typically only a modest fraction (≈15%) of brightest cluster galaxies (BCGs) show strong optical line emission, optical line emission is quite common ($71^{+9}_{-14}$%) for BGCs in cooling flow clusters (Edwards et al. 2007). Sanderson et al. (2009) find that 23 out of 24 (96%) of local cooling flow clusters with small offsets (⩽15 kpc) between their X-ray emission and BCG have optical emission lines. The line emission is presumed related to the cooling of X-ray gas at the cluster center. For the well-studied, local example of NGC 1275, the line emission is concentrated in a spectacular network of filaments extending over several arcminutes. The filaments are thought due to compressed, cooling intracluster gas within a relativistic plasma ejected by the active nucleus of NGC 1275 (Conselice et al. 2001). NGC 1275 also shows evidence of recent star formation. Understanding such systems in detail is likely important for probing the physics of feedback in massive galaxies.

### *3.4. Lensed Galaxies*

Four of the cluster galaxies observed as part of this program show additional emission lines at blue wavelengths superposed on cluster early-type spectra. These emission lines are spatially extended in three of the four sources (Figure 6). In all four sources the emission lines do not match the absorption line

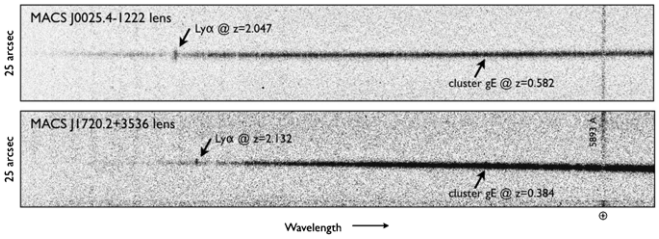


**Figure 6.** Two-dimensional processed spectra of two of the newly identified galaxy–galaxy lenses in cluster environments. Both images, obtained with the D680 grating and the blue channel of LRIS, span approximately from 2900 Å to 6150 Å in the dispersion (horizontal) axis and 25″ in the spatial (vertical) axis. Residuals from telluric NaD 5893 Å emission are visible at the long wavelength ends of the spectra. Both spectra show strong, extended Ly$\alpha$ emission superposed atop red emission from early-type members of the targeted MACS clusters.

redshift (Figure 7). The spectra are reminiscent of lenses spectroscopically identified in the SDSS luminous red galaxy sample, such as the $z = 2.7$ Einstein cross identified by Bolton et al. (2006b) and lower redshift strong lenses identified by the Sloan Lens ACS (SLACS) survey (Bolton et al. 2006a). Two of the four new lenses have publicly available, two-band Advanced Camera for Surveys (ACS) images in the *Hubble* Legacy Archive. These images, presented in Figure 8, clearly show strongly lensed background galaxies behind red, early-type galaxies. Such systems are valuable probes of the lensing galaxy mass and mass profile. L. A. Moustakas et al. (2012, in preparation) present a detailed analysis of these new systems.

## 4. SUMMARY

We present a catalog of 514 redshifts obtained in the fields of 24 galaxy clusters, including 363 early-type cluster members. Paper I derives ages for this sample and uses their ages to probe cosmological parameters using the differential age or cosmic chronometer test. The database released here will also be useful for studying the properties of galaxy clusters, modeling their mass distributions, and understanding the formation mechanism of both clusters and their constituent

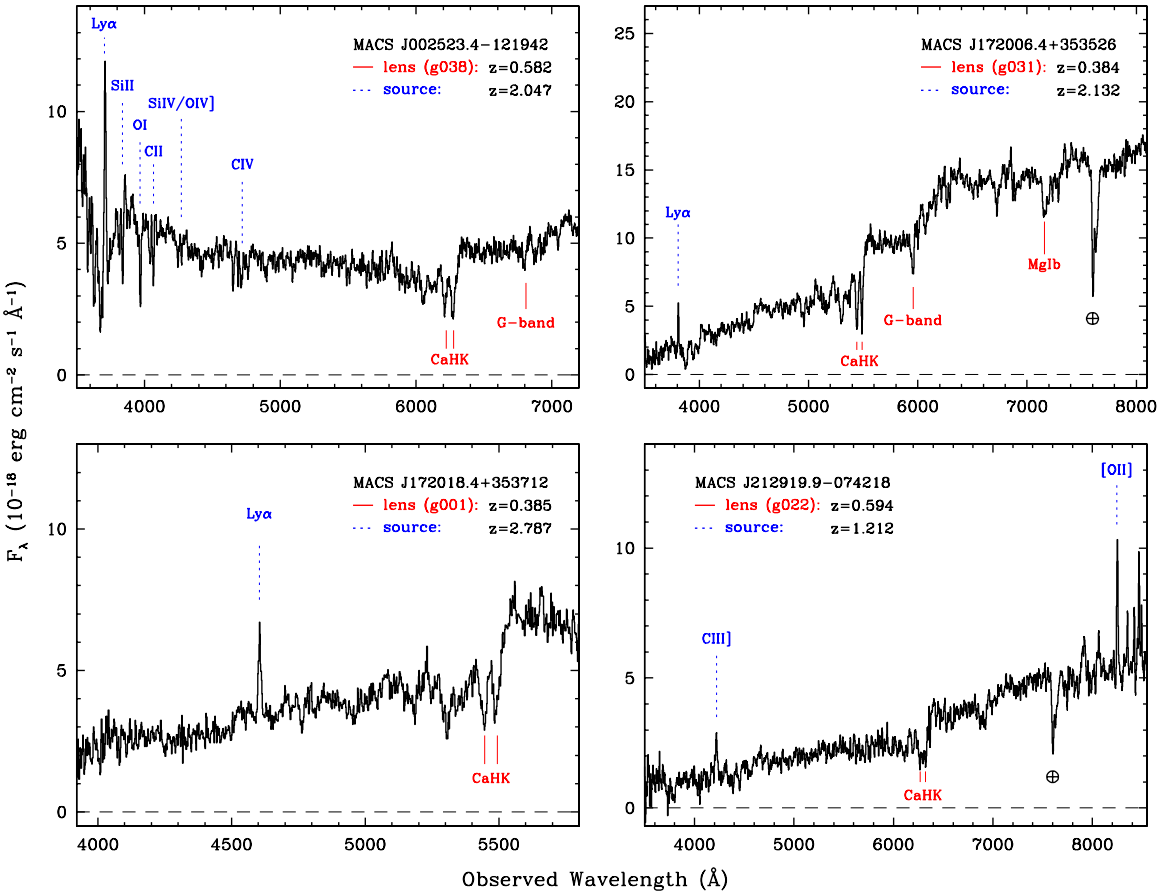


**Figure 7.** Extracted spectra of the four newly identified galaxy–galaxy lenses in cluster environments.
(A color version of this figure is available in the online journal.)


**Figure 8.** *HST*/ACS images of two of the newly identified galaxy–galaxy lenses in cluster environments. Both images, obtained from the *Hubble* Legacy Archive, are false color images created from F555W and F814W observations. Images are approximately 6″ on a side, with north up and east to the left.
(A color version of this figure is available in the online journal.)

galaxy populations. We identify three interesting central galaxies showing strong, LINER-like spectra, typical of cooling flow clusters. We also serendipitously identify four new galaxy–galaxy lenses on the outskirts of galaxy clusters.

The authors recognize and acknowledge the very significant cultural role and reverence that the summit of Mauna Kea has always had within the indigenous Hawaiian community; we are most fortunate to have the opportunity to conduct observations from this mountain. We thank M. Kasliwal for assistance with the P60 scheduling, F. Harrison and R. Griffith for assisting with the 2009 March Keck observations, L. Moustakas for useful discussions of the new gravitational lenses, and A. Barth and A. Edge for interesting discussions of the cD galaxy spectra. We also thank H. Ebeling for checking our MACS spectroscopic results against his unpublished results; in almost all cases, our

results agreed with $\Delta z \leqslant 0.004$. We are grateful to the referee for a timely and helpful report. Astrometry for two of the 2005 masks was provided by `astrometry.net` (Lang et al. 2010). The work of DS was carried out at Jet Propulsion Laboratory, California Institute of Technology, under a contract with NASA. R.J. and L.V. acknowledge support from the Spanish Ministerio de Ciencia e Innovacion and the European Union FP7 program. M.K. was supported by DoE DE-FG03-92-ER40701 and the Gordon and Betty Moore Foundation. This research made use of the NASA/IPAC Extragalactic Database (NED) which is operated by the Jet Propulsion Laboratory, California Institute of Technology, under contract with NASA. Figure 8 is based on observations made with the NASA/ESA *Hubble Space Telescope*, and obtained from the *Hubble* Legacy Archive, which is a collaboration between the Space Telescope Science Institute (STScI/NASA), the Space Telescope European Coordinating Facility (ST-ECF/ESA), and the Canadian Astronomy Data Centre (CADC/NRC/CSA).

## REFERENCES

Abell, G. O. 1958, ApJS, 3, 211
Ashby, M. L. N., et al. 2009, ApJ, 701, 428
Barcons, X., et al. 2007, A&A, 476, 1191
Becker, R. H., White, R. L., & Helfand, D. J. 1995, ApJ, 450, 559
Belloni, P., Bruzual, A. G., Thimm, G. J., & Roser, N. J. 1995, A&A, 297, 61
Belloni, P., & Roser, H. 1996, A&AS, 118, 65
Bolton, A. S., Burles, S., Koopmans, L. V. E., Treu, T., & Moustakas, L. A. 2006a, ApJ, 638, 703
Bolton, A. S., Moustakas, L. A., Stern, D., Burles, S., Dey, A., & Spinrad, H. 2006b, ApJ, 646, L45
Brinchmann, J., Kunth, D., & Durrett, F. 2008, A&A, 485, 657
Brodwin, M., et al. 2006, ApJ, 651, 791
Caldwell, R., Davé, R., & Steinhardt, P. 1998, Phys. Rev. Lett., 80, 1582
Cenko, S. B., et al. 2006, PASP, 118, 1396
Conselice, C. J., Gallagher, J. S., III, & Wyse, R. F. G. 2001, AJ, 122, 2281
Czoske, O., Kneib, J., Soucail, G., Bridges, T. J., Mellier, Y., & Cuillandre, J. 2001, A&A, 372, 391
Dorman, B., O'Connell, R. W., & Rood, R. T. 2003, ApJ, 591, 878
Dressler, A., & Gunn, J. E. 1992, ApJS, 78, 1
Dressler, A., Smail, I., Poggianti, B., Butcher, H., Couch, W., Ellis, R., & Oemler, A. 1999, ApJS, 122, 51
Dunlop, J. S., Peacock, J. A., Spinrad, H., Dey, A., Jimenez, R., Stern, D., & Windhorst, R. A. 1996, Nature, 381, 581
Ebeling, H., Barrett, E., Donovan, D., Ma, C., Edge, A. C., & Speybroeck, L. 2007, ApJ, 661, 33
Ebeling, H., Edge, A. C., & Henry, J. P. 2001, ApJ, 553, 668
Edge, A. C., Ebeling, H., Bremer, M., Röttgering, H., van Haarlem, M. P., Rengelink, R., & Courtney, N. J. D. 2003, MNRAS, 339, 913
Edwards, L. O. V., Hudson, M. J., Balogh, M. L., & Smith, R. J. 2007, MNRAS, 379, 100
Eisenhardt, P. R., et al. 2004, ApJS, 154, 48
Eisenhardt, P. R., et al. 2008, ApJ, 684, 905
Eisenstein, D. J., et al. 2001, AJ, 122, 2267
Ellingson, E., Yee, H., Abraham, R., Morris, S., & Carlberg, R. 1998, ApJS, 116, 247
Ellingson, E., Yee, H. K. C., Abraham, R. G., Morris, S. L., Carlberg, R. G., & Smecker-Hane, T. A. 1997, ApJS, 113, 1
Fanelli, M. N., O'Connell, R. W., Burstein, D., & Wu, C. C. 1992, ApJS, 82, 197
Halliday, C., et al. 2004, A&A, 427, 397
Jimenez, R., & Loeb, A. 2002, ApJ, 573, 37
Jimenez, R., Verde, L., Treu, T., & Stern, D. 2003, ApJ, 593, 622
Koester, B. P., et al. 2007, ApJ, 660, 239
Lang, D., Hogg, D. W., Mierle, K., Blanton, M., & Roweis, S. 2010, AJ, 139, 1782
Massey, P., & Gronwall, C. 1990, ApJ, 358, 344
Milvang-Jensen, B., et al. 2008, A&A, 482, 419
Moran, S. M., Ellis, R. S., Treu, T., Smail, I., Dressler, A., Coil, A. L., & Smith, G. P. 2005, ApJ, 634, 977
Moran, S. M., Ellis, R. S., Treu, T., Smith, G. P., Rich, R. M., & Smail, I. 2007a, ApJ, 671, 1503
Moran, S. M., Loh, B. L., Ellis, R. S., Treu, T., Bundy, K., & Macarthur, L. A. 2007b, ApJ, 665, 1067
Nakamura, O., Aragon-Salamanca, A., Milvang-Jensen, B., Arimoto, N., Ikuta, C., & Bamford, S. P. 2006, MNRAS, 366, 144
Oke, J. B., et al. 1995, PASP, 107, 375
Paturel, G., Garnier, R., & Prugniel, P. 2000, A&AS, 144, 475
Peebles, P. J. E., & Ratra, B. 1988, ApJ, 435, L17
Rosati, P., della Ceca, R., Norman, C., & Giacconi, R. 1998, ApJ, 492, L21
Sabra, B. M., Shields, J. C., & Filippenko, A. V. 2000, ApJ, 545, 157
Sanderson, A. J. R., Edge, A. C., & Smith, G. P. 2009, MNRAS, 398, 1698
Schawinkski, K., et al. 2007, ApJS, 173, 512
Soucail, G., Mellier, Y., Fort, B., & Cailloux, M. 1988, A&AS, 73, 471
Spinrad, H., Dey, A., Stern, D., Peacock, J. A., Dunlop, J., Jimenez, R., & Windhorst, R. A. 1997, ApJ, 484, 581
Stanford, S. A., Eisenhardt, P. R. M., Dickinson, M., Holden, B. P., & De Propis, R. 2002, ApJS, 142, 153
Stern, D., Jimenez, R., Verde, L., Kamionkowski, M., & Stanford, S. A. 2010, J. Cosmol. Astropart. Phys., JCAP02(2010)008
Treu, T., et al. 2005, ApJ, 633, 174
Yee, H. K. C., Ellingson, E., Morris, S. L., Abraham, R. G., & Carlberg, R. G. 1998, ApJS, 116, 211
Zepf, S. E., et al. 2008, ApJ, 683, L139
Ziegler, B. L., & Bender, R. 1997, MNRAS, 291, 527